

Article

Apoptotic Changes, Oxidative Stress and Immunomodulatory Effects in the Liver of Japanese Seabass (*Lateolabrax japonicus*) Induced by Ammonia-Nitrogen Stress during Keep-Live Transport

Meijie Guo ¹, Qi Yan ², Yixuan Dong ¹, Zhaoyang Ding ^{1,2,3,4} , Jun Mei ^{1,2,3,4,*}  and Jing Xie ^{1,2,3,4,*} 

¹ College of Food Science and Technology, Shanghai Ocean University, Shanghai 201306, China; m210311056@st.shou.edu.cn (M.G.); m210311057@st.shou.edu.cn (Y.D.); zyding@shou.edu.cn (Z.D.)

² National Experimental Teaching Demonstration Center for Food Science and Engineering, Shanghai Ocean University, Shanghai 201306, China; m210311047@st.shou.edu.cn

³ Shanghai Engineering Research Center of Aquatic Product Processing and Preservation, Shanghai 201306, China

⁴ Shanghai Professional Technology Service Platform on Cold Chain Equipment Performance and Energy Saving Evaluation, Shanghai 201306, China

* Correspondence: jmei@shou.edu.cn (J.M.); jxie@shou.edu.cn (J.X.); Tel.: +86-21-61900349 (J.M.); +86-21-6190-0351 (J.X.)

Simple Summary: Excreta produced by fish during preservation transport can increase ammonia-nitrogen (NH₃-N) levels in transport water and reduce survival rates. However, studies on the effects of NH₃-N stress on Japanese seabass during transport are limited. The objective of this study was to investigate the effects of NH₃-N stress on tissue damage, oxidative stress, apoptosis and immunity in Japanese seabass during transport, and to determine tolerance and response to NH₃-N toxicity. The results of this study provide insight into the impact of environmental factors on Japanese seabass during maintenance of live transport, which can be considered during transport in terms of improving the quality of transport water, among other things, to develop optimal procedures for live fish transport and improve survival rates during transport.

Abstract: This study investigated the effects of NH₃-N on antioxidant responses, histoarchitecture, and immunity of Japanese seabass (*Lateolabrax japonicus*) during keep-live transport. The findings suggest that NH₃-N stress transport alters the transcription of *P53*, *Caspase 9*, *Bcl2*, *Caspase 3* and *Bax* genes, demonstrating that NH₃-N stress can trigger the apoptotic pathway of *P53-Bax-Bcl2* and *Caspase* and induce apoptosis. NH₃-N stress transport also evoked transcriptional upregulation of inflammatory cytokines (*tumor necrosis factor α (TNF-α)*, *Toll-like receptor 3 (TLR-3)*, *nuclear factor kappa β (NF-κB)*, *interleukin 6 (IL-6)* and *interleukin 1β (IL-1β)*) and increased complement C3, C4, lysozyme (LZM) and immunoglobulin (IgM) levels, activating the innate immunological system during keep-live transport. In addition, NH₃-N stress transport altered changes in the levels of superoxide dismutase (SOD), catalase (CAT), glutathione-related enzymes, and heat shock proteins 70 and 90 in the liver, indicating that the antioxidant system and Hsp protected the cells from NH₃-N-induced oxidative stress. When excess ROS were not removed, they caused the body to respond with immunological and inflammatory responses, as well as apoptosis and tissue damage. This helps towards understanding the effect of NH₃-N levels on sea bass during keep-live transport.

Keywords: Japanese seabass; ammonia-nitrogen stress; keep-live transport; oxidative stress; immunological response



Citation: Guo, M.; Yan, Q.; Dong, Y.; Ding, Z.; Mei, J.; Xie, J. Apoptotic Changes, Oxidative Stress and Immunomodulatory Effects in the Liver of Japanese Seabass (*Lateolabrax japonicus*) Induced by Ammonia-Nitrogen Stress during Keep-Live Transport. *Biology* **2023**, *12*, 769. <https://doi.org/10.3390/biology12060769>

Academic Editor: Alberto Teodorico Correia

Received: 28 April 2023

Revised: 22 May 2023

Accepted: 23 May 2023

Published: 25 May 2023



Copyright: © 2023 by the authors. Licensee MDPI, Basel, Switzerland. This article is an open access article distributed under the terms and conditions of the Creative Commons Attribution (CC BY) license (<https://creativecommons.org/licenses/by/4.0/>).

1. Introduction

In China, Japanese seabass (*Lateolabrax japonicus*) is an economically important cultured fish. Nevertheless, high-density seabass keep-live transport causes ammonia-nitrogen

(NH₃-N) concentration to rise to dangerous levels in a short period, endangering the life of the sea bass. Higher NH₃-N levels can disturb the metabolism of organisms, cause tissue damage, lead to a decrease in immunity and the inflammatory reaction, and even kill fish [1]. At the same time, when fish have been in water with a high NH₃-N content, this will lead to the continuous accumulation of reactive oxygen species (ROS), causing oxidative stress and metabolic disorders in the biological system of fish. To combat this issue, cells form antioxidant defense systems such as the glutathione system [2,3]. The dynamic balance of GSH/GSSG is critical to the organism's defense and proper physiological condition [4]. Systematic analysis of the changes and functional regulation of glutathione in antioxidant defense can provide further insight into its role in NH₃-N stress transport. In addition, heat shock protein (Hsp) is crucial in defending the organism from stress-related damage. Hsp protects cells from stressor-induced protein dysfunction, such as ROS and hypoxia [5]. The organism's ability to tolerate NH₃-N is tightly correlated with the expression pattern and levels of Hsp [6]. Hsp levels are raised as a result of NH₃-N stress, according to earlier research [7].

Currently, there are many studies on NH₃-N stress, transport stress and combined stress of various stressors. According to Tao et al. [8], hybrid yellow catfish (*Tachysurus fulvidraco* ♀ × *Pseudobagrus vachellii* ♂) activates tlr5 in the TLR signaling pathway during transport, which affects immunological and inflammatory responses. It was also found that heat stress transport reduced the content of antioxidant enzymes including CAT, T-AOC and meat quality in rainbow trout (*Oncorhynchus mykiss*) [9]. Dual stress tends to affect organisms more adversely than a single stressor. Molayemraftar et al. [10] discovered that the combined impact of NH₃-N and nitrite is harmful to Common carp (*Cyprinus carpio*) antioxidant defenses and has negative effects on the blood. Esam et al. [11] also found that the combined stress of NH₃-N and heat affect the Nile tilapia (*Oreochromis niloticus*) more in terms of immunosuppression, oxidative stress and inflammation.

However, there is little research on how NH₃-N stress affects seabass during keep-live transport. The goal of this study was to look into the impact of NH₃-N stress on tissue damage, oxidative stress, apoptosis and immunity of Japanese seabass during keep-live transport, as well as to identify the tolerance and response to NH₃-N toxicity in terms of gene expression associated with the glutathione system and the *NF-κB* signaling pathway.

2. Materials and Methods

2.1. Experimental Fish

Japanese seabass (mean weight 400 ± 3.5 g, mean length 35 ± 1.0 cm) were obtained from the seafood market in Shanghai. The seabass were temporarily incubated in a 300 L food-grade tank in the laboratory for 36 h before transport experiments. Temporary incubation conditions were as follows: the water temperature was 20 °C, salinity was 16‰, pH was 7.5 and dissolved oxygen (DO) concentration was above 7.0 mg/L. To maintain high water quality, the water was replaced every day. After the transient period, the water was cooled from 20 to 12 °C at a rate of 3 °C/h.

2.2. Experiment to Determine LC₅₀ and Experimental Procedure:

A NH₄Cl master mix was used during the experiment to adjust the NH₃-N concentration to reach the required value for each experimental group. The range of NH₃-N concentration was obtained from the lowest concentration where no fish died in 48 h (2 mg/L) to the highest concentration where all fish died (40 mg/L) by the pre-experiment and divided logarithmically. Six concentration gradients were established—2 mg/L, 3.6411 mg/L, 6.6289 mg/L, 12.0684 mg/L, 21.9712 mg/L, and 40 mg/L. Nine fish were used in each experimental group and this was repeated three times. The number of dead Japanese seabass was recorded on the 12th, 24th, 36th and 48th h. Dead fish were removed promptly (considered dead if they were stationary and did not respond to the surrounding stimuli) and water quality management was the same as during the transient period. The LC₅₀ = 21.32 mg/L at 48 h was calculated based on the survival rate.

LC₅₀ = 21.32 mg/L was obtained for sea bass by pre-experiment. Four groups were set up in the formal experiment: a control group (CK), a low NH₃-N group (LA, 6.4 mg/L), a medium NH₃-N group (MA, 12.8 mg/L), and a high NH₃-N group (HA, 19.2 mg/L), which were equivalent to 30%, 60% and 90% of the 48 h LC₅₀, respectively (Table 1). NH₃-N concentration was measured using an NH₃-N detector (DWS-296, Shanghai Insa Scientific Instruments Co., Ltd., Shanghai, China) to achieve the specified NH₃-N levels. The fish were reared in sealed tanks with a fish-to-water ratio of 1:2. The dissolved oxygen (DO) concentration was guaranteed to exceed 7.0 mg/L, the water temperature was 20 °C, salinity was 16‰ and pH was 7.5 during transport. Live fish were simulated transport in a vibration conveyor in terms of 1 h on a class B road, followed by 5 h on a class A road. The cycles were repeated 8 times [12]. The numbers of dead fish were recorded at 0, 12th, 24th, 36th and 48th h, respectively. After 48 h transport, the surviving fish recovered for 24 h in seawater under transient conditions.

Table 1. Experimental groups and actual NH₃-N concentration.

Experimental Group	Actual NH ₃ -N Concentration (mg/L)
Control group (CK)	0.3
Low NH ₃ -N group (LA, 6.4 mg/L)	6.5
Medium NH ₃ -N group (MA, 12.8 mg/L)	11.5
High NH ₃ -N group (HA, 19.2 mg/L)	19.0

2.3. Sample Collection and Processing

Samples were taken once at the 0, 12th, 24th, 36th, and 48th h of NH₃-N exposure and at the 12th and 24th h of recovery, respectively. Eighteen fish were sampled per experimental group at a time, for a total of three replicate groups, using nine fish per replicate. The livers of sea bass were immediately removed, washed with saline and divided into two parts. One part of the liver tissue samples were immersed for 24 h and fixed for histological and TUNEL assays, the remaining samples were stored at −80 °C qPCR index determination and enzyme index measurement.

2.4. Biochemical, Immunological and Oxidation Parameters Analysis

Liver tissue samples were diluted 10 times with 0.1 M PBS and homogenized, then centrifuged at 5000× *g* for 10 min at 4 °C. The supernatant was extracted and used to determine the following indicators using commercial kits (Jiancheng Bioengineering Institute, Nanjing, China) measuring the following enzymes: SOD (A001-3-2), CAT (A001-3-2), alanine aminotransferase (ALT, C009-2-1), GST, aspartate aminotransferase (AST, C010-2-1), GSH-PX (A005-1-2), GR (A001-3-2), GSH/GSSG (A061-2-1), LZM (A050-1-1), total protein (TP, A045-2-2), immunoglobulin (IgM, H109-1-1), complement C3 (E032-1-1), complement C4 (E033-1-1), Hsp70 (H264-2-2), and Hsp90 (H264-3).

Malondialdehyde (MDA) in the liver was measured using the TBA method according to the kit (A003-1-2, Jiancheng Bioengineering Institute, Nanjing, China) instructions and in nmol/mg protein. MDA is a peroxidized lipid degradation product that condenses with thiobarbituric acid (TBA) to form a red product with a maximum absorption peak of 532 nm.

The level of ROS in the liver was detected with fluorescent probe 2',7'-dichlorofluorescein diacetate (DCFH-DA) (E004-1-1, Jiancheng Bioengineering Institute, Nanjing, China). DCFH-DA can be oxidized by esterase into strong green fluorescent substance DCF (2',7'-dichlorofluorescein) in the presence of reactive oxygen species. The liver tissue was homogenized and made into a single cell suspension. 2',7'-dichlorofluorescein yellow diacetate was added to the suspension and then incubated for 1 h at 37 °C, centrifuged for 10 min, and single cells were collected and washed in PBS solution. The excitation

wavelength of 500 nm and the fluorescence wavelength of 525 nm were used to determine the amount of ROS. These values were expressed as the following equation:

$$\text{ROS content (\%)} = \frac{\text{fluorescence intensity of treated cells}}{\text{fluorescence intensity of control}} \times 100$$

2.5. Apoptosis Detection

Samples were processed according to the method of He et al. [13]. Paraffin sections were made from liver tissue preserved in 4% formaldehyde solution. After dewaxing, hydration and cell permeation, the sections were assayed using a kit (Roche, Basel, Switzerland). TUNEL-positive cells were observed using a fluorescence microscope (Nikon, Tokyo, Japan). Positive apoptotic nuclei are green.

2.6. Histological Examination

The liver was dried, translucent, and embedded after being fixed for 24 h, and it was then sliced into 6 m slices using a slicer (Leica, Wetzlar Germany). The liver was examined under a light microscope (Leica, Wetzlar, Germany) after being stained with hematoxylin and eosin (HE). Then, the severity score is assigned to the degree and range of change: (–) no histopathology; (–) no histopathology; (+) <20% histopathology in the visual field; (++) 20–60% histopathology in the visual field; (+++) >60% histopathology in visual field [14].

2.7. Real-Time PCR

Total RNA was extracted from the liver sample using an RNA extraction solution (Xavier Biotechnology Co., Ltd., Wuhan, China). Ultramicro spectrophotometer (NanoDrop2000, Thermo Fisher Scientific, Waltham, MA, USA) was used to measure the quantity and quality of RNA. Using 10 µL of total RNA (200 ng/µL), the single-stranded cDNA was created by the directions of Servicebio® RT cDNA Synthesis Kit (G3330) (Xavier Biotechnology Co., Wuhan, China). The mRNA expression level of inflammatory factors and apoptotic genes was determined using RT-PCR. The total volume of the amplification reaction, which contained 2.0 µL of retrotranscription product (cDNA), 1.5 µL of 2.5 µM gene primer, 4.0 µL of water nuclease-free, and 7.5 µL of 2× qPCR Mix, was 15 µL. The reaction parameters were shown in Table 2. Primer sequences were designed according to the previously reported sequences (Table 3), and the $2^{-\Delta\Delta\text{ct}}$ technique was used to assess the degree of gene expression [15]. All samples were set in triplicate.

Table 2. The reaction parameters for quantitative PCR.

Stage	Temperature and Time	Process
Stage 1	95 °C, 30 s	predenaturation
Stage 2	95 °C, 15 s 60 °C, 30 s (40 cycles)	denature annealing/extension
Stage 3	65 °C → 95 °C	melting curve: every time the temperature rises by 0.5 °C, the fluorescence signal is collected

Table 3. Primer sequence for quantitative PCR.

Gene	Primer Sequence (5'–3')	Product Length (bp)	Temperature (°C)	Efficiency (%)	References
Apoptosis gene					
Actin	F: CAACTGGGATGACATGGAGAAG R: TTGGCTTTGGGGTTCAGG	200	60	101	[16]
TNF-α	F: GACTCCATAGGCAGCAAAGC R: AGAAAGTCTTGCCCTCGTCA	205	60	103.2	[17]

Table 3. Cont.

Gene	Primer Sequence (5′–3′)	Product Length (bp)	Temperature (°C)	Efficiency (%)	References
<i>IL-1β</i>	F: CTGAACATCAAGGGCACAGA R: GTTGAAGGGGACAGACCTGA	192	60	92.8	[17]
<i>IL-6</i>	F: TACAATGTCCTCCTCAAGCACG R: GCCTTTGACCTCCTCCATCAG	129	60	98.4	[18]
<i>TLR-3</i>	F: GGCCTGGATCAAATTCAAGA R: GACAGGGGACTGAATGGAGA	139	60	103	[19]
<i>NF-κB</i>	F: GAAGGTATGGGAGGAGGAGTTT R: AACCCACAGGGTCCAGAGGAAA	189	60	102	[20]
Pro-inflammatory factor <i>P53</i>	F: ACCATCCTGCTGAGCTTCAT R: GCCCAAAACAAGTCCCTCTG	178	60	95.3	[20]
<i>Caspase 3</i>	F: ATCACAGCAACTACGCCTCATTCG R: GCCTCTGCAAGCCTGGATGAAG	176	60	98.9	[17]
<i>Caspase 9</i>	F: TGCGGAGGAGGTGAACGAGAC R: CGGTTCTCGGACATGCTCAG	138	60	90.5	[17]
<i>Bax</i>	F: GCTCCAAAGGATGATAAACGAC R: AACAGTGCAACCACCCGAC	182	60	96.7	[20]
<i>Bcl2</i>	F: GTGGGGCTCTTCGCTTTTG R: CCATCCTCCTTGGCTCTGGA	191	60	95.1	[21]

3. Results

3.1. Oxidative Stress Response

The CAT, SOD, and ROS contents of each sample increased continuously with the transportation time, and the MN and HN groups had higher CAT, SOD, and ROS contents after 48 h of transportation (Figure 1). The CAT, SOD, and ROS contents of all groups decreased to the initial levels. The Hsp 70 and Hsp 90 contents of each group increased with the transport time and reached the peak after 36 h of transport, and the Hsp 70 and Hsp 90 contents of the MN and HN groups were significantly higher than those of the CK group ($p < 0.05$).

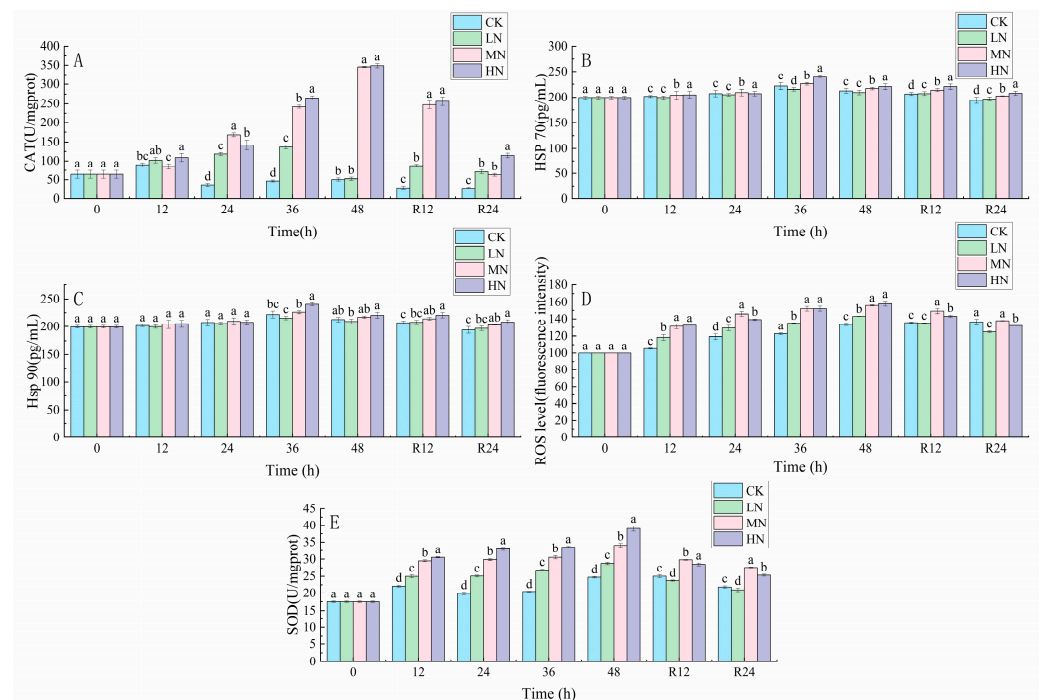


Figure 1. Changes in catalase (CAT) (A), heat stress protein 70 (Hsp 70) (B), heat stress protein 90 (Hsp90) (C), reactive oxygen species (ROS) (D) and superoxide dismutase (SOD) (E) concentrations

in the liver of Japanese seabass exposed to $\text{NH}_3\text{-N}$ of 6.4 mg/L (LA), 12.8 mg/L (MA), 19.2 mg/L (HA), and 0 mg/L (CK) for 48 h and recovered for 24 h, respectively. Values are expressed as the mean \pm S.D. Different lowercase letters indicate significant differences ($p < 0.05$) among groups. The CK $\text{NH}_3\text{-N}$ group served as the control. ($p < 0.05$, $N = 3$).

3.2. Glutathione-Related Reactions

During the recovery process, GR and GSSG contents in ammonia stress-treated samples showed a decreasing trend, while GSH contents showed an increasing trend. The contents of GSH-Px and GST in the liver of the $\text{NH}_3\text{-N}$ stress group increased with the transport time and reached the peak at 48th h. The contents of GSH-Px and GST decreased with the recovery time (Figure 2).

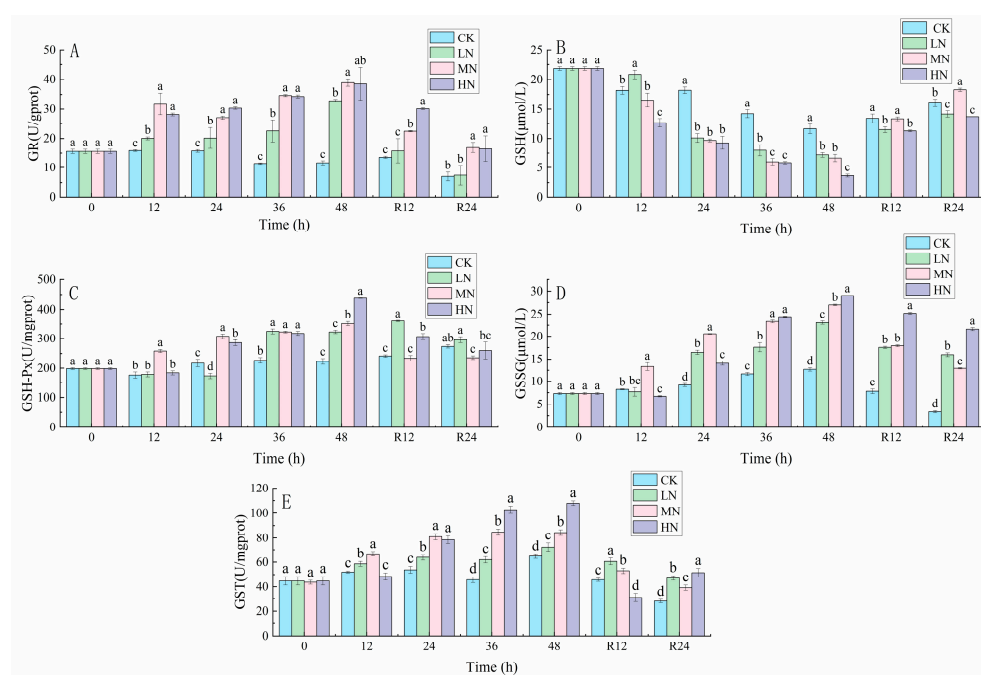


Figure 2. Changes in glutathione reductase (GR) (A), glutathione (GSH) (B), glutathione peroxidase (GSH-Px) (C), oxidized glutathione (GSSG) (D) and glutathione S-transferase (GST) (E) contents in the liver of Japanese seabass exposed to $\text{NH}_3\text{-N}$ of 6.4 mg/L (LA), 12.8 mg/L (MA), 19.2 mg/L (HA), and 0 mg/L (CK) for 48 h and recovered for 24 h, respectively. Values are expressed as the mean \pm S.D. Different lowercase letters indicate significant differences ($p < 0.05$) among groups. The CK $\text{NH}_3\text{-N}$ group served as the control. ($p < 0.05$, $N = 3$).

3.3. Tissue Damage and Liver Pathology

The results in Figure 3 show that the ALT, AST, and MDA contents of all groups increased continuously with the transportation time, and the ALT, AST, and MDA contents of the HN group were the highest after 48 h of transportation ($p < 0.05$), and the ALT, AST, and MDA contents of all groups showed a decreasing trend in the recovery period.

The liver color of the LN, MN, and LN groups was significantly darker than that of the CK after 48 h of $\text{NH}_3\text{-N}$ stress transport, especially the LN group. After 24 h of recovery, the livers of the LN, MN, and LN groups were significantly lighter compared to the 48 h of transport, but still darker compared to the CK (Figure 3).

In addition, histopathological damage of the seabass liver occurred to different degrees after 48 h of $\text{NH}_3\text{-N}$ stress transport (Table 4). The CK liver showed normal hepatocytes with the neat arrangement, normal morphology, clear and intact boundaries, and nuclei located in the center of the cells (Figure 4). Hepatic tissues in the LN and MN groups

showed hepatocyte vacuolization and hepatic sinusoidal dilatation compared with the CK (Table 4). Liver tissues in the HN group were more severely damaged, showing more hepatocyte vacuolization and hepatic sinusoidal dilatation, and the nuclei shifted to the periphery and the cell boundaries blurred.

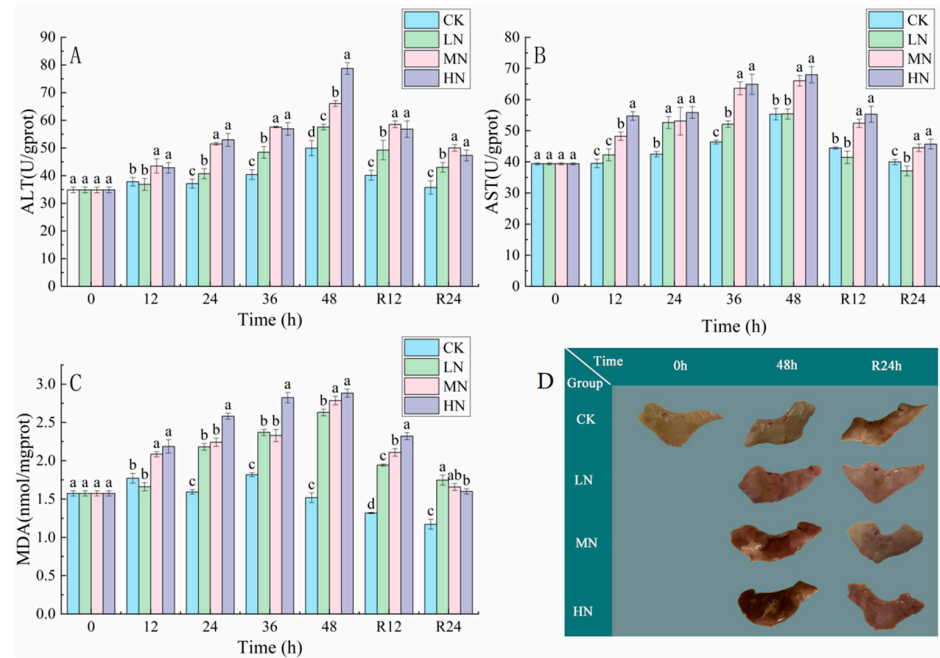


Figure 3. Changes in alanine aminotransferase (ALT) (A), aspartate aminotransferase (AST) (B), malondialdehyde (MDA) (C) and morphological of the liver (D) contents in the liver of Japanese seabass exposed to NH₃-N of 6.4 mg/L (LA), 12.8 mg/L (MA), 19.2 mg/L (HA), and 0 mg/L (CK) for 48 h and recovered for 24 h, respectively. Values are expressed as the mean ± S.D. Different lowercase letters indicate significant differences ($p < 0.05$) among groups. The CK NH₃-N group served as the control. ($p < 0.05$. $N = 3$).

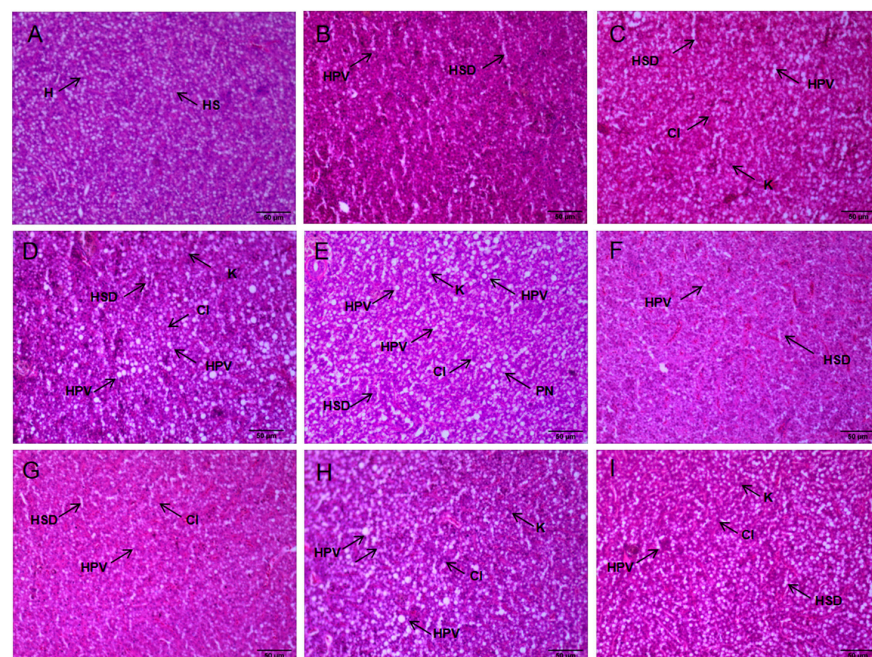


Figure 4. Paraffin sections of liver tissue were stained with HE to assess the pathological changes in different NH₃-N concentrations on Japanese seabass. Micrographs ($\times 400$) and scale bars (50 μm).

(A) represents tissue sections of the normal liver at 0 h; (B–E) represents liver tissue sections of 6.4 mg/L (LA), 12.8 mg/L (MA), 19.2 mg/L (HA), and 0 mg/L (CK) at 48th h after NH₃-N stress transport; (F–I) represents liver tissue sections of 6.4 mg/L (LA), 12.8 mg/L (MA), 19.2 mg/L (HA), and 0 mg/L (CK) at 24th h after recovery from NH₃-N stress transport. The CK NH₃-N group served as the control. (H, hepatocyte; VD, vacuolar degeneration; HS, hepatic sinusoid; HSD, hepatic sinusoid dilatation; K, karyolysis; HPV, hepatocellular vacuolation; PN, cellular peripheral nucleus; CI, cellular outline indistinguishable).

Table 4. The damage of liver records of Japanese bass transported under different NH₃-N stress was evaluated semi-quantitatively.

Time	Groups	HPV	HSD	PN	K	CI
0 h	CK	–	–	–	–	–
	CK	+	+	+	+	+
	LN	++	++	+	+	+
48 h	MN	+++	++	+	+	+
	HN	+++	+++	++	++	++
	CK	+	+	+	–	–
	LN	+	+	+	–	–
R24 h	MN	++	+	+	+	+
	HN	++	++	+	+	+

(–) no histopathology; histopathology of (+) <20% visual field; (++) 20–60% visual field histopathology; histopathology in (+++) >60% visual field. R means recovery.

3.4. Immune Response and Inflammatory Factors

The results in Figure 5 show that the contents of C3, C4, IgM, and LZM decreased continuously with the transport time. The contents of C3, C4, IgM, and LZM increased during the recovery process. After 24 h of recovery, these parameters were still lower in the HN group than in the CK.

The expressions of *TLR-3*, *NFκB*, *TNF-α*, *IL-6* and *IL-1β* were first increased and then decreased in all groups. With the increase in NH₃-N transport stress time, the expression of *TLR-3*, *NFκB*, *TNF-α*, *IL-6* and *IL-1β* in the CK and LN groups peaked at 24th h, while the gene expression of each pro-inflammatory factor in the MN and HN groups peaked at 36th h (Figure 5).

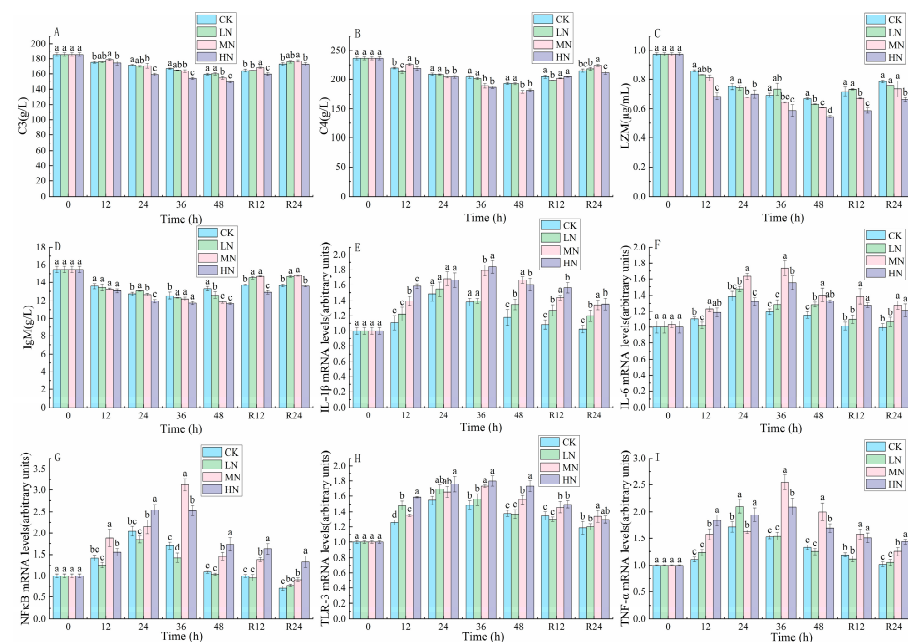


Figure 5. Changes in complement C3 (A), complement C4 (B), lysozyme (LZM) (C), immunoglobulin (IgM) (D), interleukin 1β (IL-1β) (E), interleukin 6 (IL-6) (F), nuclear factor kappa β (NF-κB) (G),

Toll-like receptor 3 (TLR-3) (H) and tumor necrosis factor α (TNF- α) (I) contents in the liver of Japanese seabass exposed to NH₃-N of 6.4 mg/L (LA), 12.8 mg/L (MA), 19.2 mg/L (HA), and 0 mg/L (CK) for 48 h and recovered for 24 h, respectively. Values are expressed as the mean \pm S.D. Different lowercase letters indicate significant differences ($p < 0.05$) among groups. The CK NH₃-N group served as the control ($p < 0.05$, $N = 3$).

3.5. Apoptosis

As shown in Figure 6, positive TUNEL signals were detected in all groups after 48 h of NH₃-N stress transport. The number of apoptotic cells was HN < MN < LN < CK. After 24 h of recovery, the number of positive cells declined in each group.

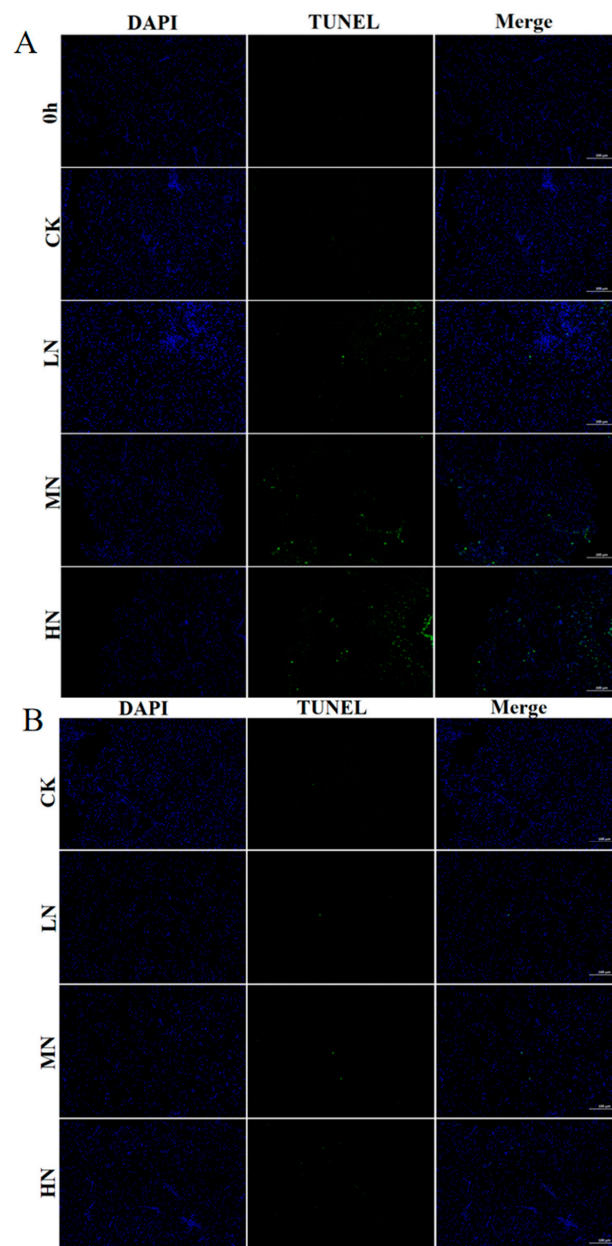


Figure 6. The TUNEL staining results of liver tissues of Japanese marine fish exposed to 6.4 mg/L (LA), 12.8 mg/L (MA), 19.2 mg/L (HA) and 0 mg/L (CK) NH₃-N concentrations in transport water at 0th h and 48th h (A) and after 24 h of recovery (B). The CK NH₃-N group served as the control.

The peak expression levels of *P53*, *Caspase 3*, *Caspase 9* and *Bax* genes in the CK and LN groups appeared at 24th h, while the peak expression levels of *P53*, *Caspase 3*, *Caspase 9* and *Bax* genes in the CK and LN groups appeared at 36th h (Figure 7).

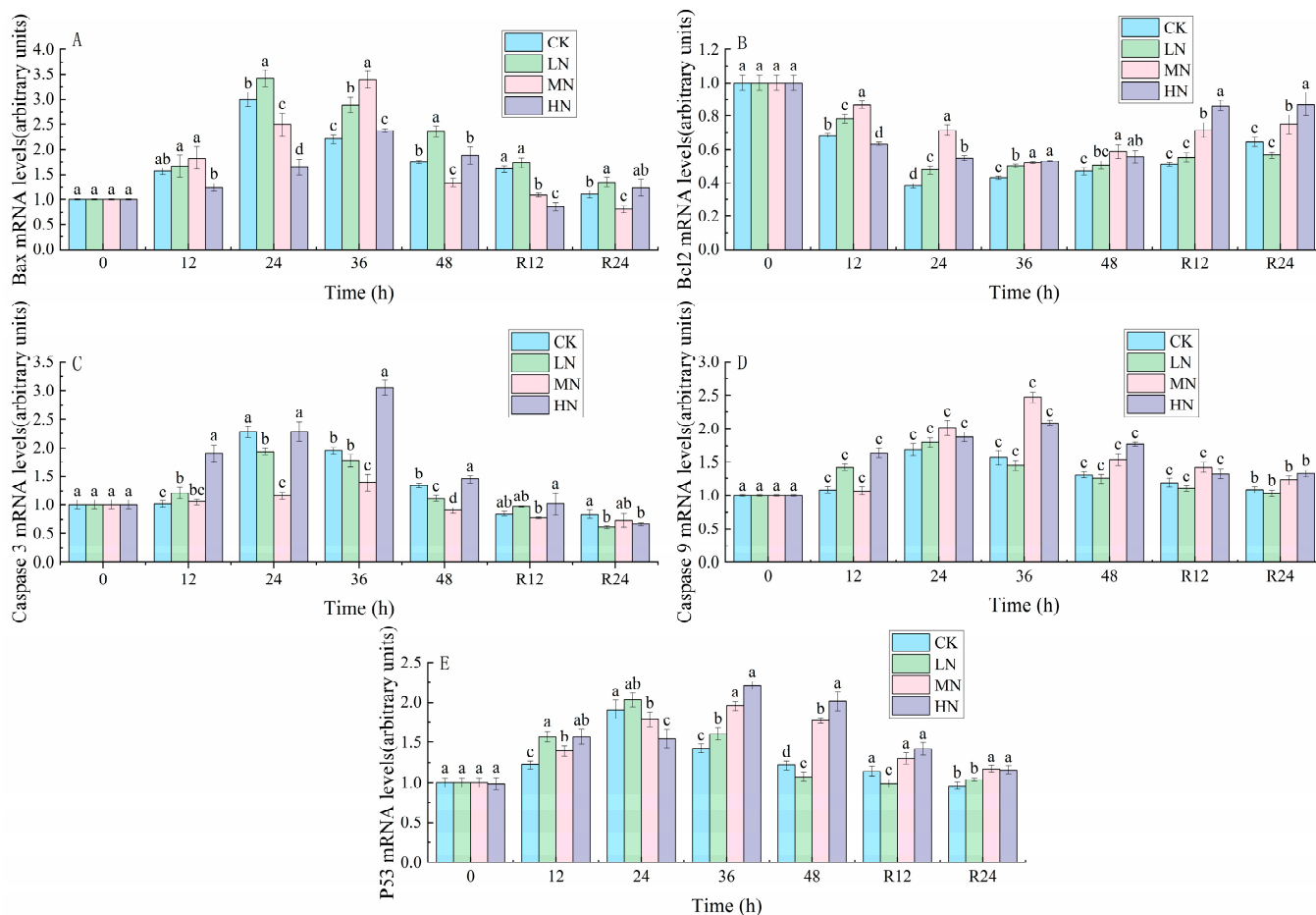


Figure 7. Changes in *Bax* (A), *Bcl2* (B), *Caspase 3* (C), *Caspase 9* (D) and *P53* (E) contents in the liver of Japanese seabass exposed to NH₃-N of 6.4 mg/L (LA), 12.8 mg/L (MA), 19.2 mg/L (HA), and 0 mg/L (CK) for 48 h and recovered for 24 h, respectively. Values are expressed as the mean \pm S.D. Different lowercase letters indicate significant differences ($p < 0.05$) among groups. The CK NH₃-N group served as the control. ($p < 0.05$, $N = 3$).

4. Discussion

4.1. The impact of NH₃-N Stress Transport on the Antioxidant Defense System of the Liver of Japanese Seabass

ROS are increased in concentration by ammonia, which causes oxidative stress in living things [1]. Organisms reduce ROS by increasing the levels of antioxidant enzymes (e.g., CAT, GST and SOD) to reduce ROS-induced oxidative damage. The initial line of defense in preventing the harm that oxidative stress causes is thought to be SOD-CAT and SOD-GPX [22]. Superoxide is converted to H₂O₂ by SOD, which is then reduced to water by CAT or GPX [23]. Because it maintains metabolic homeostasis and removes toxins, the liver is the ideal organ for assessing oxidative stress [24]. ROS produced by Japanese seabass under NH₃-N stress transport could activate its antioxidant defense system, which prevented the damage caused by NH₃-N and transport stress to the organism. A similar finding was made by Cheng et al. [1], where excessive ROS production caused by NH₃-N production resulted in increased antioxidant enzyme activity in red puffer fish. Liu et al. [14] discovered that during the start of NH₃-N stress, the juvenile golden pompano (*Trachinotus ovatus*) had an increase in antioxidant enzyme activity, and the antioxidant enzyme activity decreased

when it returned to the normal environment. ROS induced by higher $\text{NH}_3\text{-N}$ concentrations were not eliminated by the organisms after 48 h. Chen et al. [25] found that snapping turtle (*Chelydra serpentina*) exposed to high ambient $\text{NH}_3\text{-N}$ had a high level of basic antioxidant defense, that most likely relied mostly on the GSH system to eliminate extra ROS. GSH/GSSG is also considered one of the essential antioxidant systems in cells, and its stable state is crucial for maintaining the normal physiological functions of cells. $\text{NH}_3\text{-N}$ stress transport resulted in a decline in GSH content and a gradual rise in GSSG content in the liver of seabass in the current study, which is due to GSH being converted to GSSG by GSH-Px and GST in order to scavenge intracellular free radicals and peroxides, thus maintaining normal cell and tissue function and metabolism [23]. After 48 h of $\text{NH}_3\text{-N}$ stress transport, GR activity increased significantly and subsequently decreased. However, the increase in GSSG content was still higher than the decrease in GSH content, indicating that the increase in GR did not offset the GSH produced by GST and GSH-Px. After a period of recovery, GSH and GSSG did not reach their initial states and the glutathione system had not recovered for short-time equilibrium.

Molecular chaperones, such as Hsp, play an essential role in preventing cellular damage from oxidative stress by ensuring the correct folding of proteins to regulate cellular homeostasis [26]. High $\text{NH}_3\text{-N}$ promotes the production of Hsp90 and Hsp70, according to studies [27], which suggests that the buildup of too much ROS and denatured proteins causes the elevation of Hsp levels during $\text{NH}_3\text{-N}$ stress. According to the study's findings, Hsp70 and Hsp 90 levels were significantly elevated during $\text{NH}_3\text{-N}$ stress transport compared to CK. These findings are in line with the patterns of Hsp70 and Hsp90 gene expression after $\text{NH}_3\text{-N}$ exposure in kuruma shrimp (*Marsupenaeus japonicus*) and European seabass (*Dicentrarchus labrax*) [27,28]. Hsp has a key function in the prevention of protein synthesis, repair and degradation as well as apoptosis in Japanese seabass exposed to $\text{NH}_3\text{-N}$ stress. Hsp upregulation may be an effective measure to protect cells from oxidative stress [29].

4.2. The Impact of $\text{NH}_3\text{-N}$ Stress Transport on Liver Tissue Damage in Japanese Seabass

Excess ROS produced by $\text{NH}_3\text{-N}$ stress are not scavenged in time and are responsible for lipid peroxidation, inflammation and cellular damage [30]. The accumulation of ROS generates lipid peroxides (e.g., MDA) that cause cellular damage [31]. MDA levels increase after $\text{NH}_3\text{-N}$ stress transport and reflect the $\text{NH}_3\text{-N}$ generated in the liver of Japanese seabass oxidative stress, which can lead to liver damage. Peacock fish (*Poecilia reticulata*) were shown to exhibit elevated levels of ROS and MDA as well as altered antioxidant enzyme activity during $\text{NH}_3\text{-N}$ stress in a study by Zhang et al. [32]. However, the MDA content started to decrease after 24 h of recovery, showing that the harm caused by $\text{NH}_3\text{-N}$ stress transport was being gradually counteracted. After a period of recovery, the transport-induced tissue damage caused by $\text{NH}_3\text{-N}$ stress can revert to its original state.

The toxicity of a substance can be determined by measuring elevated AST and ALT activity, which are important markers of tissue damage [22,33]. Ali Taheri Mirghaed et al. [34] found the AST and ALT levels increased in common carp (*Cyprinus carpio*) after 24 h of $\text{NH}_3\text{-N}$ stress. Zhao et al. [35] found that $\text{NH}_3\text{-N}$ stress exposure resulted in elevated ALT and AST levels, indicating $\text{NH}_3\text{-N}$ stress caused tissue damage in juvenile yellow catfish (*Pelteobagrus fulvidraco*). In comparison to the CK group, the HN group's liver was much darker and more congested. $\text{NH}_3\text{-N}$ poisoning can cause changes in the color and appearance of the liver during $\text{NH}_3\text{-N}$ stress [36,37]. $\text{NH}_3\text{-N}$ stress transport resulted in hepatotoxicity, which was characterized by histopathological lesions, such as vacuolation of hepatocytes, dilated hepatic sinusoids, indistinguishable cell contours, deviated nuclei, and nuclei disintegration. The damage to liver tissue was significantly reduced through photograms and histopathological optical microscopy, but it was not enough to recover to the initial level within 48 h. This indicates that the damage caused by $\text{NH}_3\text{-N}$ toxicity is reversible. Furthermore, Yan et al. [23] found that tissue sections of bighead carp (*Aristichthys*

nobilis) after nitrite stress also revealed that liver damage caused by nitrite toxicity could be alleviated to some extent after a recovery period.

4.3. The Impact of $\text{NH}_3\text{-N}$ Stress Transport on Immunological and Inflammatory Responses in Japanese Seabass

The immunological response is a self-protective mechanism for fish against various infections. To combat infectious challenges, fish have evolved different immune systems, including lysozyme and complement. LZM and IgM maintain a healthy state in fish by eliminating invading bacteria and other pathogens while activating the complement system [38]. Studies have shown that a variety of environmental pollutants can inhibit complement C3, complement C4, IgM levels and LZM activities, thus affecting the immunological parameters of scleractinian fish [14,39]. Esam et al. [11] found the mRNA levels of complement C3 and LZM decreased, resulting in immunotoxicity when the combined ammonia-nitrogen and heat stress was applied to Nile tilapia (*Oreochromis niloticus*). In our study, complement C3, complement C4, IgM levels and LZM activities of seabass decreased after 48 h $\text{NH}_3\text{-N}$ stress transport, indicating a continued decline in immunological function. Gao et al. [40] also found that Takifugu rubripes (*T. rubripes*) showed a considerable decline in complement C3, complement C4, IgM levels and LZM activities after 12 h of $\text{NH}_3\text{-N}$ stress at different concentrations. After 24 h of recovery, the immunological parameters increased due to the weakening of oxidative stress and the gradual recovery of the immunological system from the toxic environment.

Fish that are under oxidative stress develop an inflammatory reaction. To control inflammation, TLR activation triggers the expression and release of cytokines. The results of this research concur with those of Gao et al. [41], who discovered that $\text{NH}_3\text{-N}$ exposure raised the gene level of *TLR-3* and activated the *TLR-3* signaling pathway. *TNF- α* is regarded as a crucial component of the TNF family, which causes inflammation and stimulates the immune system. The activated *TNF- α* could activate *NF- κ B* channels. *NF- κ B*, as a signaling factor, can activate several pro-inflammatory factors, including *IL-6* and *IL-1 β* . In addition, The *NF- κ B* pathway can also be activated by an excessive buildup of ROS, which can worsen the inflammatory response. Our experimental results suggest that both $\text{NH}_3\text{-N}$ stress and transport stress activated the *NF- κ B* inflammatory pathway to exert anti-inflammatory effects. This was in line with previous studies on gibel carp (*Carassius gibelio*) and guppies (*Poecilia reticulata*), where it was discovered that $\text{NH}_3\text{-N}$ stress induced the expression of genes linked to inflammation, resulting in an inflammatory response [32,42]. Furthermore, we found that the different timing of peak gene expression of anti-inflammatory factors may vary depending on the $\text{NH}_3\text{-N}$ concentration.

4.4. The Impact of $\text{NH}_3\text{-N}$ Stress Transport on Apoptosis in Japanese Seabass

In addition to inducing inflammation, oxidative stress also leads to apoptosis. The onco-gene *P53* is a crucial regulator of apoptosis, and ROS production brought on by $\text{NH}_3\text{-N}$ stress can modulate the activity of *P53*. In response to stress, *P53* alters the expression of *Bcl2* and *Bax* to induce apoptosis. The increase in the ratio of *Bax* to *Bcl2* can be used to determine the apoptosis of the organism [1]. In the current research, the *Bax/Bcl2* ratio increased in all experimental groups during $\text{NH}_3\text{-N}$ stress transport, suggesting that $\text{NH}_3\text{-N}$ stress transport could cause cell apoptosis via the *P53-Bax-Bcl2* pathway. To identify stress-induced apoptosis, Caspase expression is a crucial marker. According to Li et al. [43], that $\text{NH}_3\text{-N}$ exposure upregulated genes *Caspase 3* and *Caspase 9* and induced cell apoptosis. The current work showed that the expression of *Caspase 9* and *Caspase 3* was raised by both $\text{NH}_3\text{-N}$ exposure and transport stress, which also suggested that Caspase-dependent apoptotic pathways might be implicated in the cell death generated by transport stress of $\text{NH}_3\text{-N}$.

The results of TUNEL staining showed green fluorescent spots, which verified the hypothesis that $\text{NH}_3\text{-N}$ stress transport leads to apoptosis. The *P53-Bax/Bcl2* apoptotic route and the Caspase-dependent apoptotic pathway may both be affected by $\text{NH}_3\text{-N}$ stress in

Yellow catfish (*Pelteobagrus fulvidraco*) [36]. This is in line with what the current experimental study's findings show. These findings also imply that oxidative stress and inflammation may be intimately related to cell apoptosis brought on by simultaneous exposure to these two stressors.

5. Conclusions

This research was the first to investigate the influence of NH₃-N on oxidative stress, apoptosis, tissue damage and immunological response in Japanese seabass during keep-live transport. The histopathological and TUNEL results confirmed that ammonia and nitrogen stress during transport could produce ROS, resulting in oxidative stress, and that eliminated ROS through the glutathione system, but this system failed to provide adequate protection when exposed to highly oxidizing conditions. Excess ROS was involved in NH₃-N stress-induced apoptosis through the *P53-Bax-Bcl2* pathway and the cysteine-dependent apoptosis pathway and induced an inflammatory response via the *NF-κB* pathway. These defenses declined during the recovery period, but did not return to the normal levels compared to CK. The findings of this research help towards a thorough understanding of how environmental factors effect seabass during keep-live transport, which helps towards developing optimal procedures for transport and improving the survival rate during transport.

Author Contributions: Conceptualization, M.G. and Q.Y.; formal analysis, M.G., Q.Y., Y.D. and J.M.; funding acquisition, J.X.; investigation, Q.Y.; methodology, M.G., Y.D. and Z.D.; project administration, J.X.; resources, J.M.; software, M.G. and Z.D.; supervision, J.X.; writing—original draft, M.G.; writing—review and editing, J.M. and J.X. All authors have read and agreed to the published version of the manuscript.

Funding: The research was supported by the Agriculture Research System of China (CARS-47) and National Key R&D Program of China (2019YFD0901601).

Institutional Review Board Statement: The experimental procedures were approved by the Animal Care and Use Committee of Shanghai Ocean University (SHOU-DW-2022-059).

Informed Consent Statement: Not applicable.

Data Availability Statement: The data presented in this study are available upon request from the corresponding author.

Conflicts of Interest: The authors attest that there are no conflict of interest concerning this paper.

References

1. Cheng, C.-H.; Yang, F.-F.; Ling, R.-Z.; Liao, S.-A.; Miao, Y.-T.; Ye, C.-X.; Wang, A.-L. Effects of ammonia exposure on apoptosis, oxidative stress and immune response in pufferfish (*Takifugu obscurus*). *Aquat. Toxicol.* **2015**, *164*, 61–71. [[CrossRef](#)] [[PubMed](#)]
2. Wang, Y.; Wang, B.; Liu, M.; Jiang, K.; Wang, M.; Wang, L. Aflatoxin B1 (AFB1) induced dysregulation of intestinal microbiota and damage of antioxidant system in pacific white shrimp (*Litopenaeus vannamei*). *Aquaculture* **2018**, *495*, 940–947. [[CrossRef](#)]
3. Hodkovicova, N.; Chmelova, L.; Sehonova, P.; Blahova, J.; Doubkova, V.; Plhalova, L.; Fiorino, E.; Vojtek, L.; Vicenova, M.; Siroka, Z.; et al. The effects of a therapeutic formalin bath on selected immunological and oxidative stress parameters in common carp (*Cyprinus carpio*). *Sci. Total Environ.* **2019**, *653*, 1120–1127. [[CrossRef](#)] [[PubMed](#)]
4. Schafer, F.Q.; Buettner, G.R. Redox environment of the cell as viewed through the redox state of the glutathione disulfide/glutathione couple. *Free Radic. Biol. Med.* **2001**, *30*, 1191–1212. [[CrossRef](#)] [[PubMed](#)]
5. Kim, J.-H.; Kim, S.K.; Hur, Y.B. Temperature-mediated changes in stress responses, acetylcholinesterase, and immune responses of juvenile olive flounder *Paralichthys olivaceus* in a bio-floc environment. *Aquaculture* **2019**, *506*, 453–458. [[CrossRef](#)]
6. Liu, B.; Jia, R.; Huang, B.; Lei, J. Interactive effect of ammonia and crowding stress on ion-regulation and expression of immune-related genes in juvenile turbot (*Scophthalmus maximus*). *Mar. Freshw. Behav. Physiol.* **2017**, *50*, 179–194. [[CrossRef](#)]
7. Xu, Z.; Cao, J.; Qin, X.; Qiu, W.; Mei, J.; Xie, J. Toxic Effects on Bioaccumulation, Hematological Parameters, Oxidative Stress, Immune Responses and Tissue Structure in Fish Exposed to Ammonia Nitrogen: A Review. *Animals* **2021**, *11*, 3304. [[CrossRef](#)]
8. Zheng, T.; Song, Z.; Tao, Y.; Qiang, J.; Ma, J.; Lu, S.; Xu, P. Transport stress induces innate immunity responses through TLR and NLR signaling pathways and increases mucus cell number in gills of hybrid yellow catfish (*Tachysurus fulvidraco* ♀ × *Pseudobagrus vachellii* ♂). *Fish Shellfish Immunol.* **2022**, *127*, 166–175. [[CrossRef](#)]
9. Wu, Y.; You, X.; Sun, W.; Xiong, G.; Shi, L.; Qiao, Y.; Wu, W.; Li, X.; Wang, J.; Ding, A.; et al. Insight into acute heat stress on meat qualities of rainbow trout (*Oncorhynchus mykiss*) during short-time transportation. *Aquaculture* **2021**, *543*, 737013. [[CrossRef](#)]

10. Molayemraftar, T.; Peyghan, R.; Razi Jalali, M.; Shahriari, A. Single and combined effects of ammonia and nitrite on common carp, *Cyprinus carpio*: Toxicity, hematological parameters, antioxidant defenses, acetylcholinesterase, and acid phosphatase activities. *Aquaculture* **2022**, *548*, 737676. [[CrossRef](#)]
11. Esam, F.; Khalafalla, M.M.; Gewaily, M.S.; Abdo, S.; Hassan, A.M.; Dawood, M.A.O. Acute ammonia exposure combined with heat stress impaired the histological features of gills and liver tissues and the expression responses of immune and antioxidative related genes in Nile tilapia. *Ecotoxicol. Environ. Saf.* **2022**, *231*, 113187. [[CrossRef](#)] [[PubMed](#)]
12. Wang, Q.; Mei, J.; Cao, J.; Xie, J. Effects of *Melissa officinalis* L. Essential Oil in Comparison with Anaesthetics on Gill Tissue Damage, Liver Metabolism and Immune Parameters in Sea Bass (*Lateolabrax maculatus*) during Simulated Live Transport. *Biology* **2022**, *11*, 11. [[CrossRef](#)] [[PubMed](#)]
13. He, K.; Luo, X.; Wen, M.; Wang, C.; Qin, C.; Shao, J.; Gan, L.; Dong, R.; Jiang, H. Effect of acute ammonia toxicity on inflammation, oxidative stress and apoptosis in head kidney macrophage of *Pelteobagrus fulvidraco* and the alleviation of curcumin. *Comp. Biochem. Physiol. Part C Toxicol. Pharmacol.* **2021**, *248*, 109098. [[CrossRef](#)] [[PubMed](#)]
14. Liu, M.-J.; Guo, H.-Y.; Zhu, K.-C.; Liu, B.-S.; Liu, B.; Guo, L.; Zhang, N.; Yang, J.-W.; Jiang, S.-G.; Zhang, D.-C. Effects of acute ammonia exposure and recovery on the antioxidant response and expression of genes in the Nrf2-Keap1 signaling pathway in the juvenile golden pompano (*Trachinotus ovatus*). *Aquat. Toxicol.* **2021**, *240*, 105969. [[CrossRef](#)]
15. Livak, K.J.; Schmittgen, T.D. Analysis of Relative Gene Expression Data Using Real-Time Quantitative PCR and the $2^{-\Delta\Delta CT}$ Method. *Methods* **2001**, *25*, 402–408. [[CrossRef](#)]
16. Tan, P.; Dong, X.; Xu, H.; Mai, K.; Ai, Q. Dietary vegetable oil suppressed non-specific immunity and liver antioxidant capacity but induced inflammatory response in Japanese sea bass (*Lateolabrax japonicus*). *Fish Shellfish Immunol.* **2017**, *63*, 139–146. [[CrossRef](#)]
17. Huang, H.; Zhang, X.; Liang, X.; Wu, X.; Gu, X.; Han, J.; Xue, M. N-carbamoylglutamate improves lipid metabolism, inflammation, and apoptosis responses in visceral adipocytes of Japanese seabass (*Lateolabrax japonicus*), in vivo and in vitro. *Anim. Nutr.* **2021**, *7*, 707–715. [[CrossRef](#)]
18. Li, X.; Sun, J.; Wang, L.; Song, K.; Lu, K.; Zhang, L.; Ma, X.; Zhang, C. Effects of dietary vitamin E levels on growth, antioxidant capacity and immune response of spotted seabass (*Lateolabrax maculatus*) reared at different water temperatures. *Aquaculture* **2023**, *565*, 739141. [[CrossRef](#)]
19. Fan, H.; Wang, L.; Wen, H.; Wang, K.; Qi, X.; Li, J.; He, F.; Li, Y. Genome-wide identification and characterization of toll-like receptor genes in spotted sea bass (*Lateolabrax maculatus*) and their involvement in the host immune response to *Vibrio harveyi* infection. *Fish Shellfish Immunol.* **2019**, *92*, 782–791. [[CrossRef](#)]
20. Xiang, Y.; Jia, P.; Liu, W.; Yi, M.; Jia, K. Comparative transcriptome analysis reveals the role of p53 signalling pathway during red-spotted grouper nervous necrosis virus infection in *Lateolabrax japonicus* brain cells. *J. Fish Dis.* **2019**, *42*, 585–595. [[CrossRef](#)]
21. Le, Y.; Jia, P.; Jin, Y.; Liu, W.; Jia, K.; Yi, M. The antiviral role of heat shock protein 27 against red spotted grouper nervous necrosis virus infection in sea perch. *Fish Shellfish Immunol.* **2017**, *70*, 185–194. [[CrossRef](#)] [[PubMed](#)]
22. Zhang, H.; Wang, Q.; Dong, Y.; Mei, J.; Xie, J. Effects of tricaine methanesulphonate (MS-222) on physiological stress and fresh quality of sea bass (*Lateolabrax maculatus*) under simulated high-density and long-distance transport stress. *Biology* **2023**, *12*, 223. [[CrossRef](#)] [[PubMed](#)]
23. Lin, Y.; Miao, L.-H.; Pan, W.-J.; Huang, X.; Deng, J.M.; Zhang, W.-X.; Ge, X.-P.; Liu, B.; Ren, M.-C.; Zhou, Q.-L.; et al. Effect of nitrite exposure on the antioxidant enzymes and glutathione system in the liver of bighead carp, *Aristichthys nobilis*. *Fish Shellfish Immunol.* **2018**, *76*, 126–132. [[CrossRef](#)] [[PubMed](#)]
24. Abdel-Latif, H.M.R.; Shukry, M.; El Euony, O.I.; Mohamed Soliman, M.; Noreldin, A.E.; Ghetas, H.A.; Dawood, M.A.O.; Khallaf, M.A. Hazardous Effects of SiO₂ Nanoparticles on Liver and Kidney Functions, Histopathology Characteristics, and Transcriptomic Responses in Nile Tilapia (*Oreochromis niloticus*) Juveniles. *Biology* **2021**, *10*, 183. [[CrossRef](#)]
25. Chen, X.; Li, M.; Niu, C. Diverse defense responses to ammonia stress in three freshwater turtles. *Aquaculture* **2022**, *546*, 737302. [[CrossRef](#)]
26. Cui, Y.; Zhao, N.; Wang, C.; Long, J.; Chen, Y.; Deng, Z.; Zhang, Z.; Zhao, R.; Sun, J.; Wang, Z.; et al. Acute ammonia stress-induced oxidative and heat shock responses modulated by transcription factors in *Litopenaeus vannamei*. *Fish Shellfish Immunol.* **2022**, *128*, 181–187. [[CrossRef](#)]
27. Sinha, A.K.; Zinta, G.; AbdElgawad, H.; Asard, H.; Blust, R.; De Boeck, G. High environmental ammonia elicits differential oxidative stress and antioxidant responses in five different organs of a model estuarine teleost (*Dicentrarchus labrax*). *Comp. Biochem. Physiol. Part C Toxicol. Pharmacol.* **2015**, *174*, 21–31. [[CrossRef](#)]
28. Ou, H.; Liang, J.; Liu, J. Effects of acute ammonia exposure on oxidative stress, endoplasmic reticulum stress and apoptosis in the kuruma shrimp (*Marsupenaeus japonicus*). *Aquac. Rep.* **2022**, *27*, 101383. [[CrossRef](#)]
29. Li, X.; Liu, S.; Wang, Y.; Lu, W.; Zhang, Q.; Cheng, J. Genomic and Transcriptomic Landscape and Evolutionary Dynamics of Heat Shock Proteins in Spotted Sea Bass (*Lateolabrax maculatus*) under Salinity Change and Alkalinity Stress. *Biology* **2022**, *11*, 353. [[CrossRef](#)]
30. Elshopakey, G.E.; Mahboub, H.H.; Sheraiba, N.I.; Abduljabbar, M.H.; Mahmoud, Y.K.; Abomughaid, M.M.; Ismail, A.K. Ammonia toxicity in Nile tilapia: Potential role of dietary baicalin on biochemical profile, antioxidant status and inflammatory gene expression. *Aquac. Rep.* **2023**, *28*, 101434. [[CrossRef](#)]

31. Bian, C.; Yu, H.; Yang, K.; Mei, J.; Xie, J. Effects of single-, dual-, and multi-frequency ultrasound-assisted freezing on the muscle quality and myofibrillar protein structure in large yellow croaker (*Larimichthys crocea*). *Food Chem. X* **2022**, *15*, 100362. [[CrossRef](#)] [[PubMed](#)]
32. Zhang, C.; Ma, J.; Qi, Q.; Xu, M.; Xu, R. Effects of ammonia exposure on anxiety behavior, oxidative stress and inflammation in guppy (*Poecilia reticulata*). *Comp. Biochem. Physiol. Part C Toxicol. Pharmacol.* **2023**, *265*, 109539. [[CrossRef](#)] [[PubMed](#)]
33. Shi, A.; Ma, H.; Shi, X.; Zhou, W.; Pan, W.; Song, Y.; Chen, Q.; Yu, X.; Niu, C.; Yang, Y.; et al. Effects of microbe-derived antioxidants on growth, digestive and aminotransferase activities, and antioxidant capacities in the hepatopancreas of *Eriocheir sinensis* under ammonia nitrogen stress. *Aquac. Fish.* **2023**, *in press*. [[CrossRef](#)]
34. Taheri Mirghaed, A.; Paknejad, H.; Mirzargar, S.S. Hepatoprotective effects of dietary Artemisia (*Artemisia annua*) leaf extract on common carp (*Cyprinus carpio*) exposed to ambient ammonia. *Aquaculture* **2020**, *527*, 735443. [[CrossRef](#)]
35. Zhao, H.; Peng, K.; Wang, G.; Mo, W.; Huang, Y.; Cao, J. Metabolic changes, antioxidant status, immune response and resistance to ammonia stress in juvenile yellow catfish (*Pelteobagrus fulvidraco*) fed diet supplemented with sodium butyrate. *Aquaculture* **2021**, *536*, 736441. [[CrossRef](#)]
36. Sun, Z.; Wang, S.; Zhang, M.; Jiang, H.; Li, M. Chronic toxicity study of ammonia exposure in juvenile yellow catfish *Pelteobagrus fulvidraco*. *Aquaculture* **2023**, *567*, 739266. [[CrossRef](#)]
37. Zhang, M.; Wang, S.; Sun, Z.; Jiang, H.; Qian, Y.; Wang, R.; Li, M. The effects of acute and chronic ammonia exposure on growth, survival, and free amino acid abundance in juvenile Japanese sea perch *Lateolabrax japonicus*. *Aquaculture* **2022**, *560*, 738512. [[CrossRef](#)]
38. Chen, W.; Gao, S.; Huang, Y.; Chang, K.; Zhao, X. Addition of Chlorella sorokiniana meal in the diet of juvenile rainbow trout (*Oncorhynchus mykiss*): Influence on fish growth, gut histology, oxidative stress, immune response, and disease resistance against *Aeromonas salmonicida*. *Fish Shellfish Immunol.* **2022**, *129*, 243–250. [[CrossRef](#)]
39. Gao, X.-Q.; Fei, F.; Huo, H.H.; Huang, B.; Meng, X.S.; Zhang, T.; Liu, B.-L. Impact of nitrite exposure on plasma biochemical parameters and immune-related responses in *Takifugu rubripes*. *Aquat. Toxicol.* **2020**, *218*, 105362. [[CrossRef](#)]
40. Gao, X.; Wang, X.; Wang, X.; Fang, Y.; Cao, S.; Huang, B.; Chen, H.; Xing, R.; Liu, B. Toxicity in *Takifugu rubripes* exposed to acute ammonia: Effects on immune responses, brain neurotransmitter levels, and thyroid endocrine hormones. *Ecotoxicol. Environ. Saf.* **2022**, *244*, 114050. [[CrossRef](#)]
41. Gao, X.-Q.; Fei, F.; Huang, B.; Meng, X.S.; Zhang, T.; Zhao, K.-F.; Chen, H.-B.; Xing, R.; Liu, B.-L. Alterations in hematological and biochemical parameters, oxidative stress, and immune response in *Takifugu rubripes* under acute ammonia exposure. *Comp. Biochem. Physiol. Part C Toxicol. Pharmacol.* **2021**, *243*, 108978. [[CrossRef](#)] [[PubMed](#)]
42. Wu, L.; Chen, Q.; Dong, B.; Han, D.; Zhu, X.; Liu, H.; Yang, Y.; Xie, S.; Jin, J. Resveratrol attenuated oxidative stress and inflammatory and mitochondrial dysfunction induced by acute ammonia exposure in gibel carp (*Carassius gibelio*). *Ecotoxicol. Environ. Saf.* **2023**, *251*, 114544. [[CrossRef](#)] [[PubMed](#)]
43. Li, M.; Zhang, M.; Qian, Y.; Shi, G.; Wang, R. Ammonia toxicity in the yellow catfish (*Pelteobagrus fulvidraco*): The mechanistic insight from physiological detoxification to poisoning. *Fish Shellfish Immunol.* **2020**, *102*, 195–202. [[CrossRef](#)] [[PubMed](#)]

Disclaimer/Publisher's Note: The statements, opinions and data contained in all publications are solely those of the individual author(s) and contributor(s) and not of MDPI and/or the editor(s). MDPI and/or the editor(s) disclaim responsibility for any injury to people or property resulting from any ideas, methods, instructions or products referred to in the content.